Scientia Iranica C (2022) 29(3), 1377–1390

Sharif University of Technology
Scientia Iranica
Transactions C: Chemistry and Chemical Engineering
http://scientiairanica.sharif.edu

Sensitivity analysis of electromagnetic stimulation of oil wells using simulation technique and Box-Behnken design

S. Karami and A.H. Saeedi Dehaghani*

Department of Petroleum Engineering, Faculty of Chemical Engineering, Tarbiat Modares University, Tehran, Iran.

Received 30 May 2020; received in revised form 18 April 2021; accepted 30 January 2022

KEYWORDS
Electromagnetic wave;
Brine water;
Frequency;
Salinity;
Box-Behnken;
Dielectric constant.

Abstract. This research aims to investigate the parameters affecting the electromagnetic (EM) stimulation of an oil well. To this end, a simulator and Box-Behnken design were implemented to determine the sensitivity of EM stimulation with respect to rock and fluid properties. Seven factors of the frequency, brine water salinity, water saturation, oil dielectric constant, rock dielectric constant, porosity, and initial temperature were analyzed through 62 simulation runs. The dielectric constants of brine water were obtained using the Stogryn model as a function of brine salinity, frequency, and initial temperature. Based on the distance far from the wellbore, the wellbore region was divided into four sections: 5–6, 6–10, 10–20, and 20–100 cm. The most affecting parameter in the domain of 5–20 cm is brine salinity. The frequency and water saturation were obtained as the next affecting parameters, respectively. The most affecting parameter in the section of 20–100 cm is the frequency. In the section of 20–10 cm, the second and third affecting parameters were found to be brine water salinity and water saturation, respectively. The highest power loss density in the 5–6 cm section was obtained as 4300 Watt/m^3 while the highest density was almost 1 Watt/m^3 in the section of 20–100 cm.

1. Introduction

Increasing global demands for energy sources, such as fossil fuels, has motivated petroleum engineers to seek new methodologies for facilitating oil production from heavy oil reservoirs [1]. One of the new methods, which is widely used in the production of viscous oil, is the wellbore electromagnetic (EM) stimulation. The EM waves are generated by the periodical oscillation of the electric and the magnetic field. The EM waves are familiar due to their applications in telecommunication and power generation affairs. They transfer the energy in the forms of supplied force in the electric and magnetic fields. Also, they are subjected to attenuation while propagating in the medium. Dissipation of the EM wave leads to heat generation in the medium [2]. These waves have some characteristics such as frequency, wavelength, and amplitude. The frequency only depends on the source frequency and does not change due to medium electrical properties. The wavelength of the EM wave is attributed as the shortest distance between two points with an identical phase. The velocity of the EM wave could be found by multiplying the frequency by the wavelength [2].

*. *Corresponding author. Tel./Fax: +98 21 82883350*
E-mail address: asaeedi@modares.ac.ir (A.H. Saeedi Dehaghani)

doi: 10.24200/sci.2022.56072.4537

Through the propagation of the EM waves into the medium, the electric and magnetic energy, stored in the EM wave, dissipates in the medium due to dielectric loss.

According to Eqs. (1) and (2), the dissipation of energy depends on frequency, radian frequency, dielectric constant, loss factor, and root mean square electric field intensity [3,4]:

$$p_{ave} = \omega \varepsilon_0 \bar{\varepsilon} E^2 V, \tag{1}$$

$$p_{ave} = \sigma E^2, \tag{2}$$

where the parameters of σ, ω, ε_0, $\bar{\varepsilon}$, E, P_{ave}, and V stand for electric conductivity, radian frequency, dielectric constant (real part), dielectric constant (imaginary part), root mean square electric field, average dissipated power, and the volume of the media [3]. Hence, moisture content, temperature, organic materials, water saturation, and mineral-bound water affect the final result of the EM heating due to their potential in changing the dielectric properties of the medium [5].

According to Eqs. (1) and (2), it is obvious that the material properties of the medium affect the efficiency of EM heating, strongly. Hence, the cases of EM heating of sands, clays, coals, heavy oil, light one, and brine water have different efficiencies due to various dielectric behaviors. Despite the conventional heating which homogeneously heats the material, the EM heating increases the material temperature based on their electrical properties, leading to the creation of hotspot zones [4,6,7]. The selective microwave heating of the oil crude led to the desorption of the polar compounds, such as asphaltene molecules from the aged rock surface [8,9].

The EM heating of oil wells, which has been accepted as a successful method of oil well stimulation for decades, has some effects on the rock and fluid properties. Changing the oil viscosity is one of the reasons why EM stimulation is implemented in the oil wells. By applying the EM stimulation, the oil viscosity reduces to a minimum value due to the visbreaking of long-chain hydrocarbons [10]. Increasing the exposure time comes to increasing the viscosity due to the domination of gas expelling. The addition of nanomaterials such as Fe, titanium oxide, and super activated carbon reduces the optimum time for viscosity reduction [10–12]. Moreover, the EM waves reduce the asphaltene content and asphaltene size of the heavy oil sample [6].

Many researchers suggested using the EM waves for recovery and stimulation of the oil shale. Hascakir and Akin suggested the hybrid of the microwave (a portion of the EM wave spectrum) and conventional heating [13]. They found microwave heating to be rapidly influencing while conventional heating very stable, hence proposing a combination of both. Pyrolysis of the Moroccan oil shales under microwave irradiation was investigated by Harfi et al. [14]. They found that oil sample from pyrolysis seems more maltenic, less polar, and contains less sulfur and nitrogen than the oils produced by the conventional method. Ali et al. investigated the scattering parameters of sandstone saturated with brine and nanofluids. Zinc oxide and Bismuth ferrite nanoparticles were used to find their potential to enhance oil recovery. Based on the EM properties reported by the vector network analyzer, maximum absorption, dielectric permittivity, and magnetic permeability were observed in bismuth ferrite nanoparticles [15]. Simultaneous implementation of nanoparticles and the EM wave is one of the novel hybrid methods used for enhanced oil recovery. In this hybrid method, magnetic nanoparticles such as Al_2O_3, SiO_2, CeO_2, TiO_2, NiO, ZnO, Ni, Fe, $Y_3Fe_5O_{12}$, and ZrO_2 are activated by the magnetic field to propagate in the reservoir medium. The effects of the parameters such as particle size, composition, and wave frequency have been studied comprehensively [15–20].

The mineral content of the porous media influences the efficiency of EM heating, strongly. Robinson et al. related the mineral content of tar sands to the efficiency of EM wave heating [21]. They concluded that the microwave treatment was feasible for low-grade tar sands. Besides, the hydrated clays improved microwave heating.

This research aims to determine the sensitivity of the EM heating regarding the dielectric constants of the materials, wave frequency, salinity, porosity, and initial temperature. In the rest of the study, the model structure and properties are discussed.

2. Model description

Computer Simulation Technology (CST) software was implemented to simulate the oil well subjected to the EM stimulation/heating. CST software is a tool to simulate the behavior of the EM waves. It simulates the structures and the EM waves by discretizing the structure and solving the Maxwell equations in each cell. Solving the Maxwell equations which are shown in Eqs. (3)–(6) is the fundamental of the CST software:

$$\nabla \times E = j\omega \mu H, \tag{3}$$

$$\nabla \times H = -j\omega \varepsilon_r \bar{\varepsilon} E, \tag{4}$$

$$\nabla \times E = 0, \tag{5}$$

$$\nabla \times H = 0. \tag{6}$$

In Eqs. (3)–(6), the parameters of E, j, ω, μ, H, ε_r, and $\bar{\varepsilon}$ represent the electric field (V/m), current density (A/m^2), angular frequency (rad/s), magnetic

permeability (H/m), magnetic field (T), the relative dielectric constant, imaginary dielectric constant, and power loss density (Watt), respectively. To find the electric and magnetic fields, the structure was discretized into cells via CST software and the Maxwell equations were solved through numerical iteration methods [22,23].

To model the near-wellbore structure, two coaxial cylinders were set to simulate the oil well and near the wellbore region. The inner cylinder with a radius of 5 cm and a height of 100 cm is considered as the oil well. The outer cylinder with a radius of 100 cm and height of 100 cm stands for the near-wellbore region. A metallic rectangular cube port with dimensions of 2 cm × 2 cm × 10 cm was placed at the center of the oil well to radiate the EM waves. The power loss of the EM waves was reported at radii of 5–6 cm, 6–10 cm, 10–20 cm, and 20–100 cm. Discretized structure of the oil well and the near-wellbore region is shown in Figure 1. It should be mentioned that the boundary condition was open on the boundaries of the investigated regions (r = 100 cm) to allow the EM waves to leave the investigated region.

The average EM properties of the oil, brine water, and rock were attributed to the electric property of the near-wellbore region. The parameters of water saturation, water salinity, frequency, oil dielectric constant, rock dielectric constant, temperature, and porosity were considered as affecting factors of the EM stimulation/heating. The Box-Behnken design was employed to investigate the sensitivity analysis of the EM stimulation for seven factors at two levels. According to the Box-Behnken design of seven factors at two levels, 62 runs were performed to find the sensitivity analysis. The list of parameters including upper and lower levels is shown in Table 1.

The oil dielectric constant depends on the dielectric constant of the organic compounds. For example, the dielectric constants of normal pentane, toluene, and stearic acid are 1.76, 2.38, and 1.7. Besides, the existence of more polar compounds, such as asphaltene and resin molecules, leads to a higher dielectric constant based on the chemistry and concentration of the polar compound. To cover a wide range of the oil dielectric constants, 1–3 was selected for simulations [24,25]. Goual studied the impedance spectroscopy of the oil in two conditions: containing asphaltene and without asphaltene particles [25]. It was reported that the dielectric constants of the oil remained constant at

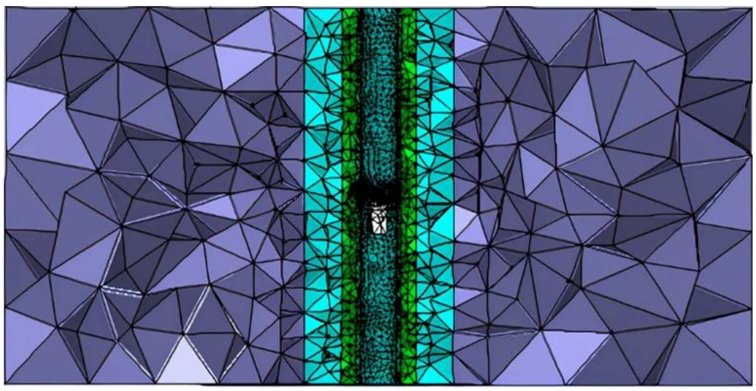

Figure 1. A view of discretized port and near oil-well region with four sections of 5–6 cm, 6–10 cm, 10–20 cm, and 20–100 cm far from the center of the wellbore.

Table 1. Seven affecting factors with minimum and maximum values.

Parameter	Factor	Unit	Type	Minimum	Maximum
Water saturation	S_w	Dimensionless	Numeric	0	1
Water salinity	S	g/L	Numeric	0.1	100
Frequency	F	Hz	Numeric	10^3	10^8
Oil dielectric constant	E_o	Dimensionless	Numeric	1	3
Rock dielectric constant	E_r	Dimensionless	Numeric	3	7
Initial temperature	T_i	°C	Numeric	50	90
Porosity	Phi	Dimensionless	Numeric	0.05	0.3

frequencies higher than 1 kHz; hence, considering the electric constants of oil unchanged at frequencies higher than 1000 Hz seems reasonable. The dielectric constants of $MgCO_3$, $CaCO_3$, and SiO_2, which are predominant minerals in the reservoir rock texture, are 7.12, 9.2, and 3.88, respectively [4,26]. In other research papers, the dielectric constant of a dry clean sandstone was found to be almost 2.6 [27] and the dielectric constant of limestone was in the range of 5–7 in the wave frequency used in this study [28]. To cover the sandstone and limestone formations, the dielectric constant range is set to be 3–7. Based on the wellbore production or injection condition, water saturation and salinity occur in a wide range. The authors tried to cover all possible conditions for an oil well, which is subjected to low-salinity water injection, producing formation water, or any other process that affects the wellbore water salinity or saturation. For this purpose, the saturation is considered to be in the range of 0–1.

The dielectric constant of brine water is a strong function of the frequency, salinity, and temperature, and it is not as simple as the rock and the oil one. Stogryn model [29], which is shown in Eqs. (7)-(17), was used to evaluate the dielectric constants of the brine water:

$$\varepsilon = \varepsilon_\infty + \frac{\varepsilon_0 - \varepsilon_\infty}{1 - i2\pi\tau f} + \frac{i\sigma}{2\pi\varepsilon_0^* f}, \tag{7}$$

$$\varepsilon_0 = \varepsilon_0(T,0)a(N,T), \tag{8}$$

$$2\tau\pi(T,N) = 2\pi\tau(T,0)b(N,T), \tag{9}$$

$$a(N) = 1.000 - 0.2551N + 5.15110^{-2}N^2 - 6.88910^{-3}N^3, \tag{10}$$

$$b(N,T) = 0.146310^{-2}NT + 1.000 - 0.04896N - 0.02967N^2 + 5.64410^{-3}N^3, \tag{11}$$

$$\varepsilon_0(T,0) = 87.74 - 0.40008T + 9.39810^{-4}T^2 + 1.41010^{-6}T^3, \tag{12}$$

$$2\pi\tau(T,0) = 1.110910^{-14} - 3.82410^{-12}T + 6.93810^{-14}T^2 - 5.09610^{-16}T^3, \tag{13}$$

$$N = S(1.70710^{-10} + 1.20510^{-5}S + 4.05810^{-9}S^2), \tag{14}$$

$$\sigma(25,N) = N \times (10.394 - 2.3776 \times N + 0.68258 \times N^2 - 0.13538 \times N^3 + 1.0086 \times 10^{-2} \times N^4), \tag{15}$$

$$D = 25 - T, \tag{16}$$

$$\sigma(T,N) = \sigma(25,N) \times (1 - 1.962 \times 10^{-2} \times D + 8.08 \times 10^{-5} \times D^2 - (3.02 \times 10^{-5} + 3.92 \times 10^{-5} \times D) + N \times (1.721 \times 10^{-5} - 6.584 \times 10^{-6} \times D)), \tag{17}$$

where:

ε_0	The static constant of the brine water
ε_∞	Optical dielectric constant of the brine
τ	Relaxation time (s)
ε_0^*	Permittivity of the electric field at free space that is 8.85×10^{-12} (F/m)
σ	Ionic conductivity of brine water (mho/m)
f	Frequency of EM waves (Hz)
S	Salinity in parts per thousand (g/L)

As could be seen from Eq. (7), the conductivity and optical dielectric constant of the brine water should be calculated. The optical dielectric constant of materials was obtained by tending the operating frequency to infinite. The optical dielectric constant of brine water in the case of different salinities and temperatures could be calculated by the Meissner model, which is shown in Eqs. (18) and (19) [30]:

$$\varepsilon_0(T, S=0) = a_1 + a_2T, \tag{18}$$

$$\varepsilon_\infty(T,S) = \varepsilon_\infty(T, S=0) \cdot (1 + S(a_3 + a_4T)), \tag{19}$$

where a_1, a_2, a_3, and a_4 are 3.6143, 2.8841×10^{-2}, -2.04265×10^{-3}, and 1.57883×10^{-4}, respectively.

Sensitivity analysis of seven factors of water saturation, brine water salinity, frequency, temperature, oil dielectric constant, rock dielectric constant, and porosity was investigated using the Box-Behnken method at two levels. The power loss of the EM waves was set as the target of analysis. In the rest of this study, the power loss equations of the EM waves at four investigation radii of 5–6 cm, 6–10 cm, 10–20 cm, and 20–100 cm are discussed.

3. Result and discussion

To find the power loss density, the ratio of EM wave dissipation power per volume of the section was used to explain the EM heating.

3.1. Power loss at 5–6 cm

The consistency of actual simulation data with the proposed correlation suggested by the Box-Behnken design is shown in Figure 2. The adjusted R^2 value of the

correlation is 0.92; hence, the model seems valid to explain the dependency of the power loss regarding seven parameters in the section of 5–6 cm far from the oil well.

Eq. (20) shows the regression correlation proposed by Box-Behnken. As is clear from the terms in this equation, the most affecting parameter in the efficiency of EM heating is the brine water salinity. In terms of significance, other effective parameters are frequency and saturation. The porosity and initial temperature of the near-wellbore region are in the next order of affecting factors. Besides, the least important parameters include the rock and oil dielectric constants. In other words, all of the seven factors improve the EM heating, but in different orders. According to Eq. (20), the porosity and initial temperature of the wellbore seem to be more effective than the rock and oil type (dielectric constants of the oil and rock).

$$\begin{aligned}\text{Power loss density (5–6)} &= 420.778 + 517.628 \times S_w \\ &+ 753.027 \times S + 541.517 \times F + 0.353695 \times E_o \\ &+ 20.6821 \times E_r + 121.81 \times T_i + 345.889 \times \phi \\ &+ 712.012 \times S_w S + 431.895 \times S_w F - 0.0050304 \\ &\times S_w E_o + 3.75032 \times S_w E_r + 96.4139 \times S_w T_i \\ &+ 284.992 \times S_w \phi + 751.062 \times SF - 0.0050304 \\ &\times SE_o + 57.2165 \times SE_r + 162.97 \times ST_i \\ &+ 448.9 \times S\phi + 1.00562 \times FE_o + 3.7504 \times FE_r \\ &+ 163.038 \times FT_i + 303.738 \times F\phi - 0.00261653 \\ &\times E_o E_r + 0.0746707 \times E_o F + 1.10088 \times E_o \phi \\ &+ 0.615199 \times E_r T_i - 54.2376 \times E_r \phi \\ &+ 65.349 \times T_i \phi - 25.0898 \times S_w^2 + 328.501 \\ &\times S^2 + 10.7587 \times F^2 - 12.1275 \times E_o^2 \\ &+ 25.4563 \times E_r^2 - 8.07331 \times T_i^2 + 21.3049 \times \phi. \end{aligned} \quad (20)$$

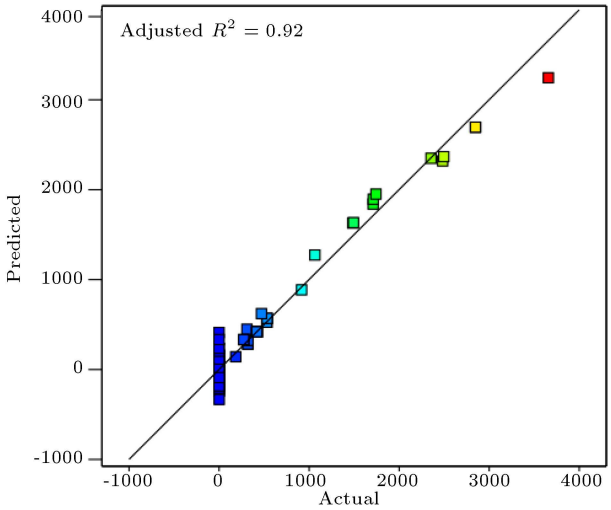

Figure 2. Predicted versus actual data of the power loss density 5–6 cm far from the wellbore.

Figure 3 represents the three-dimensional surface of the power loss density versus salinity and saturation of the brine water at different frequencies. The other four factors remained constant in the middle of their range. According to Figure 3, the frequency strongly affects the efficiency of power. The highest power loss among the frequencies of 1 kHz, 10 kHz, 100 kHz, and 10 MHz is almost 1000 Watt/m^3, and there is no notable improvement in the power loss of the EM heating. The highest power loss density increases to almost 1300 Watt/m^3 and 4300 Watt/m^3 at the frequencies of 10 MHz and 100 MHz, respectively. Moreover, there is a minor enhancement of power loss density as the saturation tends to 0. It may be due to the reduction of the effect of brine water dielectric conformation at lower water saturation. Reduction of the brine water saturation leads to increased oil saturation and it enhances the EM heating at lower frequencies.

3.2. Power loss at 6–10 cm

Figure 4 shows the consistency of actual simulation data of EM heating at the radius of 6–10 cm far from the oil well with the proposed correlation suggested by the Box-Behnken design. The adjusted R^2 value of the correlation is 0.95. Therefore, the model seems consistent with the actual data.

Eq. (21) is the regression correlation, which fits with the power loss density of the EM waves at the radius of 6–10 cm far from the oil well. Similar to Eq. (21), the most affecting parameter on the EM heating is the salinity of the brine water. In terms of significance, other effective parameters are frequency and saturation. All of the investigated parameters enhance the performance of EM heating method, each with different degrees. Similar to the 5–6 cm section, porosity and initial temperature improve the EM heating more than oil and rock dielectric constants.

$$\begin{aligned}\text{Power loss density (6–10)} &= 141.923 + 162.594 \times S_w \\ &+ 223.717 \times S + 175.183 \times F + 0.465199 \times E_o \\ &+ 7.61005 \times E_r + 33.7473 \times T_i + 106.807 \times \phi \\ &+ 206.934 \times S_w S + 148.307 \times S_w F - 0.0014381 \\ &\times S_w E_o + 28.2118 \times S_w T_i + 90.2329 \times S_w \phi \\ &+ 223.823 \times SF - 0.0014381 \times SE_o + 18.5298 \end{aligned}$$

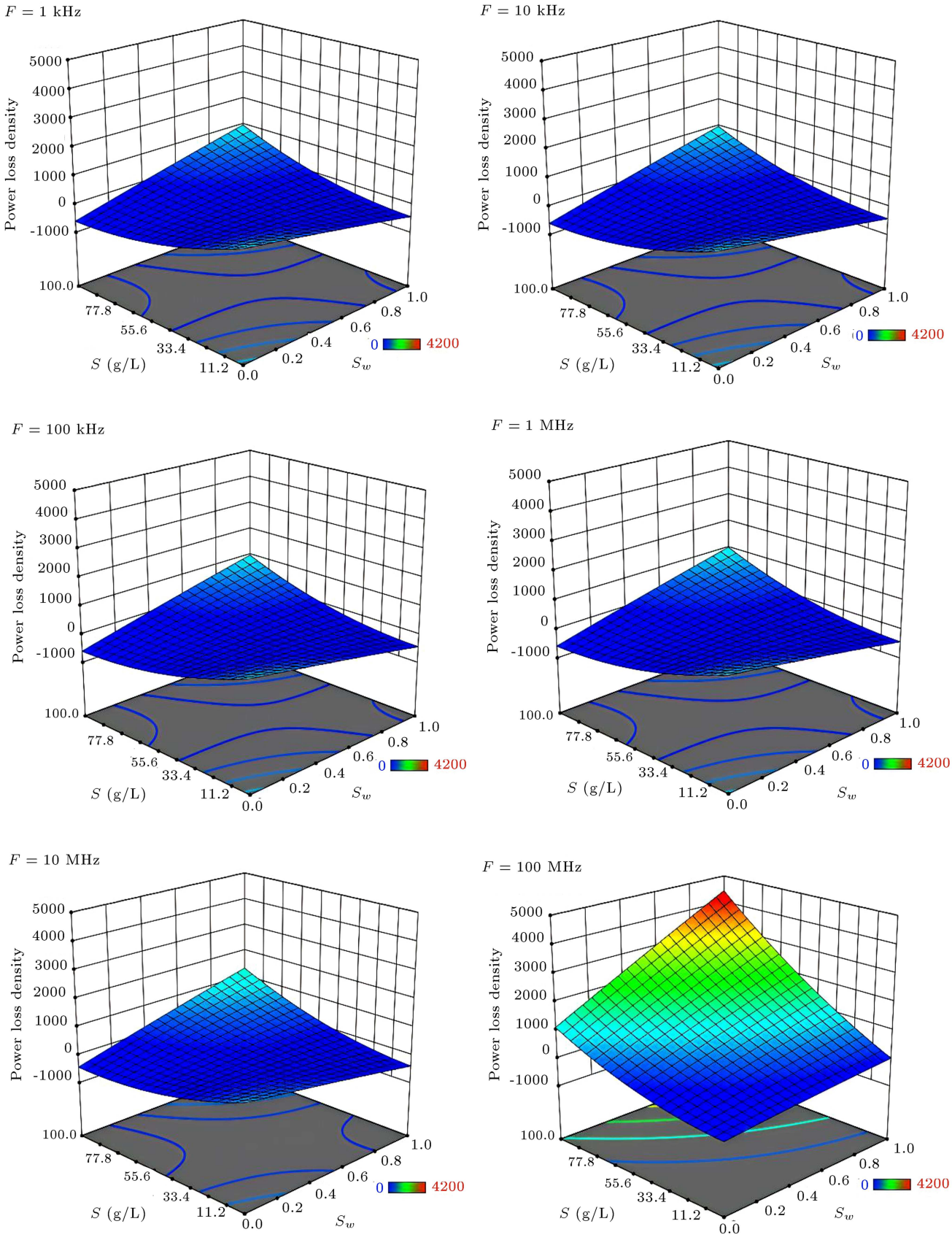

Figure 3. Three-dimensional view of the power loss density in 5–6 cm versus salinity and water saturation at different frequencies.

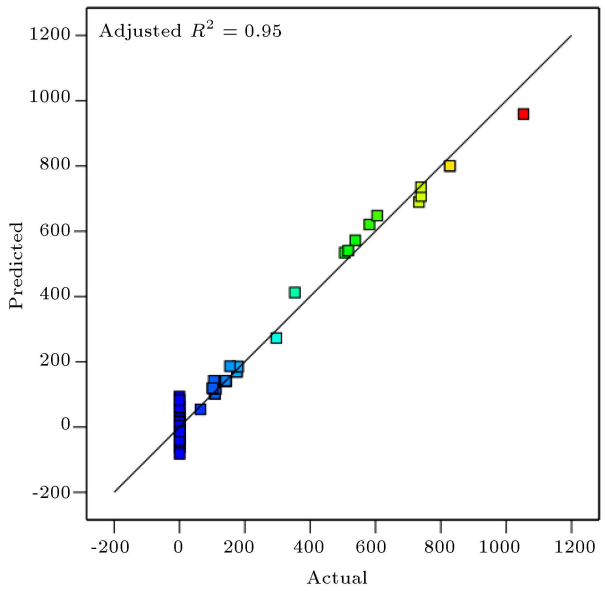

Figure 4. Predicted versus actual data of the power loss density 6–10 cm far from the wellbore.

$$\times SE_r + 39.2071 \times ST_i + 127.674 \times S\phi + 1.32736 \times E_oF + 2.98819 \times FE_r + 39.2322 \times FT_i + 102.501 \times F\phi - 0.00197801 \times E_oE_r + 0.0310908 \times E_oT_i + 1.34228 \times \phi E_o + 0.315448 \times E_rT_i - 16.9304 \times E_r\phi + 18.0544 \times T_i\phi - 11.545 \times S_w^2 + 80.3317 \times S^2 + 7.34369 \times F^2 - 3.75741 \times E_o^2 + 10.5879 \times E_r^2 - 5.42022 \times T_i^2 + 7.56306 \times \phi. \quad (21)$$

Figure 5 shows the power loss density of the EM waves at the radius of 6–10 cm far from the oil well. The 3-dimensional graphs of the power loss density are sketched versus brine water saturation and salinity. The maximum power loss density was obtained as almost 1350 Watt/m^3 at a frequency of 100 MHz, and the highest power loss density at a frequency of 1 kHz found almost 250 Watt/m^3. Hence, the ratio of the highest power loss at the highest to the one at the lowest frequency is 5.4. The 3-dimensional graph anomalies of power loss density in the 6–10 cm section are similar to those in the 5–6 cm section. The most important note about Figure 5 is its lower EM power loss density than the power loss density in the section of 5–6 cm.

3.3. Power loss at 10–20 cm

Figure 6 shows the consistency of correlation suggested by Box-Behnken method with the data of the EM stimulation at 10–20 cm far from the wellbore. The adjusted R^2 value at 0.96 confirms the consistency of the correlation with the simulation data.

Eq. (22) represents the relation between the sensitivity of the EM wave power loss and seven affecting parameters. Similar to Eqs. (20) and (21), the most affecting parameter is the salinity of brine water. The frequency and the brine water saturation are the next affecting factors. All of the factors improve the power loss density of EM stimulation.

$$\text{Power loss density (10–20)} = 22.6463 + 20.5467 \times S_w + 23.2719 \times S + 23.175 \times F + 0.963918 \times E_o + 1.40951 \times E_r + 2.65549 \times T_i + 13.3261 \times \phi + 19.8503 \times SS_w + 23.1872 \times FS_w - 0.000136412 \times S_wE_o + 1.1393 \times S_wE_r + 2.53642 \times S_wT_i + 11.4381 \times \phi S_w + 23.0898 \times SF - 0.000136412 \times SE_o + 2.46676 \times SE_r + 0.891994 \times ST_i + 10.5972 \times S\phi + 2.85849 \times E_oF + 1.13931 \times FE_r + 0.897966 \times FT_i + 17.9403 \times F\phi + 0.000116534 \times E_oE_r + 2.85849 \times E_oF + 1.13931 \times E_rF + 0.897966 \times FT_i + 17.9403 \times F\phi + 0.000116534 \times E_oE_r + 0.00623108 \times E_oT_i - 2.36292 \times \phi E_o + 0.0718212 \times E_rT_i - 2.10078 \times E_r\phi + 1.00237 \times T_i\phi. \quad (22)$$

Figure 7 shows a 3-dimensional view of the power loss density versus salinity and saturation at different frequencies at 10–20 cm far from the wellbore. The behavior of power loss in the section of 10–20 cm is similar to those at 5–6 cm and 6–10 cm. The highest power loss density occurs at the highest brine water saturation and salinity. The power loss increases at a frequency of 100 MHz, drastically. The highest power loss density at a frequency of 100 MHz is almost 10 folds of the highest power loss density at a frequency of 1 kHz. The ratio of the highest power loss density at the maximum and minimum frequencies in Sections 5–6 cm and 6–10 cm was obtained as 4.3 and 5.4, respectively. Therefore, the dependency of the power loss density on the operating frequency increases upon increasing the investigation radius.

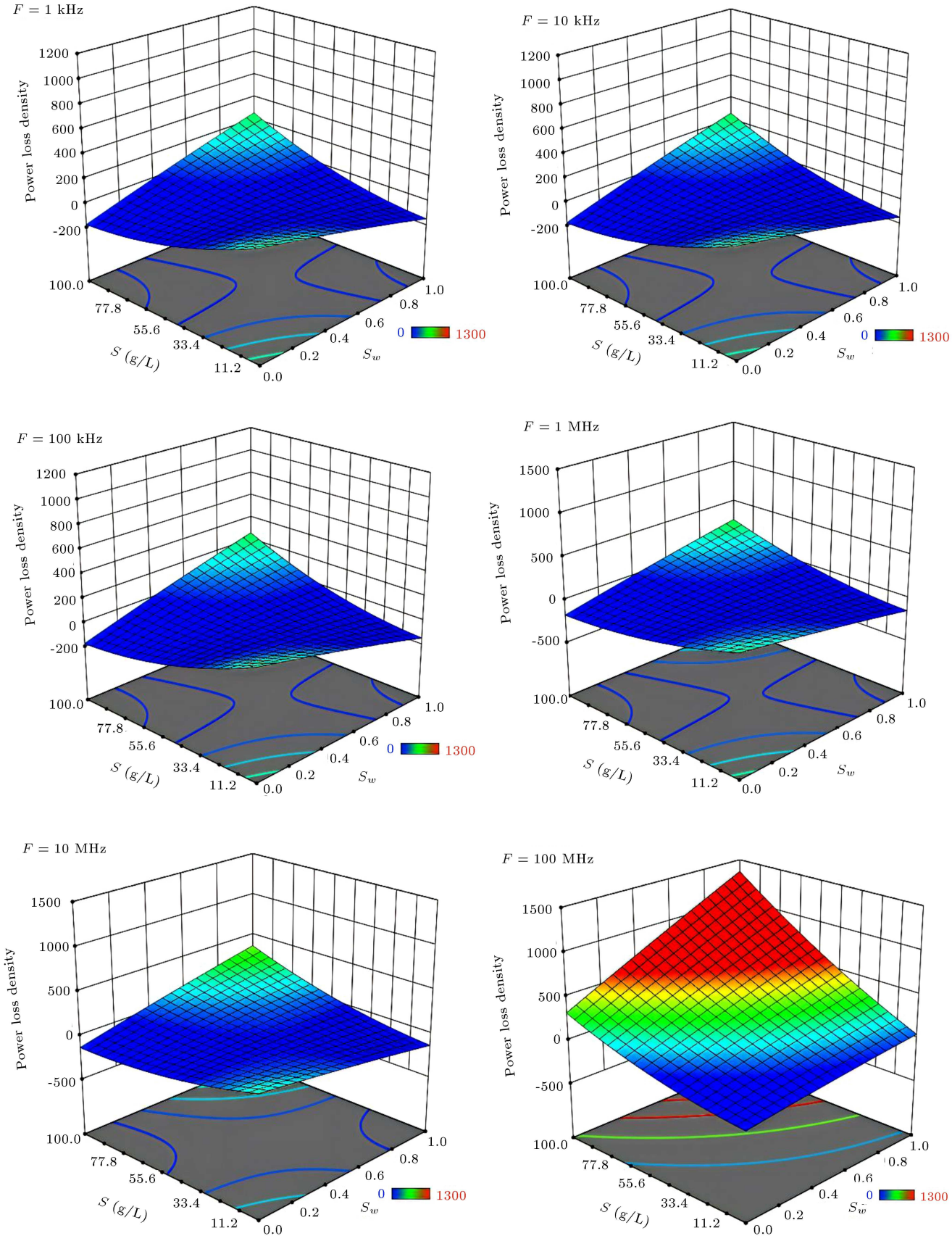

Figure 5. Three-dimensional view of the power loss density at 6–10 cm versus salinity and water saturation at different frequencies.

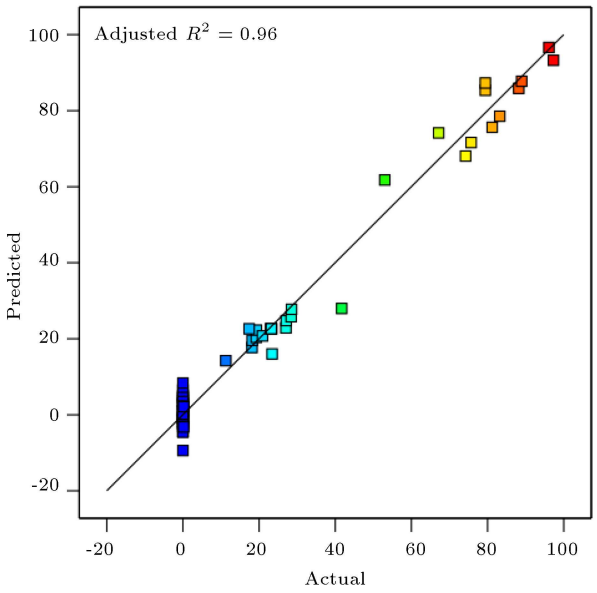

Figure 6. Predicted versus actual data of the power loss density at 10–20 cm far from the wellbore.

3.4. Power loss at 20–100 cm

Figure 8 shows the comparison of actual and predicted data of the EM stimulation in the section of 20–100 cm far from the oil well. The adjusted R^2 of the prediction correlation was obtained as 0.69. Hence, the correlation corresponding to the section of 20–100 cm shows less consistency concerning the previous sections.

Eq. (23) shows the correlation of the power loss density of the EM waves concerning affecting parameters. The most affecting factor that has a higher coefficient is the frequency. It implies a contrast between the affecting levels in the sections of 5–20 cm and 20–100 cm far from the wellbore. It could be explained by skin law, which is shown as in Eq. (24) [31].

$$\begin{aligned}\text{Power loss density (20–100)} &= 0.400502 + 0.182326 \\ &\times S_w + 0.116576 \times S + 0.27495 \times F + 0.00165029 \\ &\times E_o + 0.0241823 \times E_r - 0.00825269 \times T_i \\ &+ 0.0366213 \times \phi + 0.0731587 \times SS_w + 0.262691 \\ &\times S_w F - 5.02563 \times 10^{-7} \times \times S_w E_o + 0.0281251 \\ &\times S_w E_r - 0.0110051 \times S_w + 0.0612681 \times \phi S_w \\ &+ 0.102412 \times SF - 5.02612 \times 10^{-7} \times SE_o \\ &+ 0.0146805 \times SE_r - 0.0300912 \times ST_i \\ &- 0.014303 \times S\phi + 0.00337948 \times E_o F + 0.028125 \\ &\times E_r F - 0.029203 \times FT_i + 0.0627647 \times F\phi \\ &+ 8.66466 \times 10^{-5} \times E_o E_r - 9.66121 \times 10^{-5} \\ &\times E_o T_i + 0.0020807 \times \phi E_o - 0.00262026 \times E_r T_i \\ &- 0.0113828 \times E_r \phi - 0.0253635 \times \phi T_i \\ &- 0.140165 \times S_w^2 + 0.234609 \times S^2 - 0.00120913 \\ &\times F^2 + 0.0476178 \times E_o^2 + 0.00357479 \times E_r^2 \\ &- 0.054252 \times T_i^2 + 0.00484721 \times \phi^2. \end{aligned} \tag{23}$$

Skin law explains that the penetration depth of the EM waves highly depends on the frequency of the EM waves [31]. Penetration of the EM wave into the materials is reduced by increasing the frequency. This fact becomes more important when the EM wave behavior is investigated at further depths in the reservoir. In terms of significance, the next affecting factors are brine water saturation and salinity. In contrast to all of the previous sections, the initial temperature had a negative coefficient.

$$\delta_s = (\omega\mu\sigma)^{-0.5}. \tag{24}$$

Figure 9 represents the power loss density in the section of 20–100 cm far from the wellbore, which is the lowest in the entire investigation region. The most power loss density at a frequency of 1 kHz is almost 0.135 Watt/m^3 and it occurs at saturation and salinity rates of 0.35 and 0.46 g/L. In contrast to the other sections closer to the wellbore, at the lower frequency, the highest power loss density is obtained in the middle of the 3-dimensional graphs, not at the edges close to the highest salinity and saturation. It could be explained by Eq. (23) which recognizes the frequency as the most effective factor in the power loss density distribution. The most power loss density happens at a frequency of 100 MHz where the saturation and salinity are almost 1 and 100 g/L, respectively.

4. Conclusion

A sensitivity analysis was implemented by using Box-Behnken design, the Stogryn model, and Computer Simulation Technology (CST) software to investigate the affecting parameters of the electromagnetic (EM) stimulation of the oil wells. The seven factors include the frequency, the salinity of brine water, saturation, oil dielectric constant (oil type), rock dielectric constant (rock type), porosity, and initial temperature of wellbore region. Following the 62 runs performed by the CST software, the following outcomes are presented:

1. From 5–20 cm far from the wellbore, the most effective parameter in the EM heating of oil wells is the salinity of brine water. The frequency of

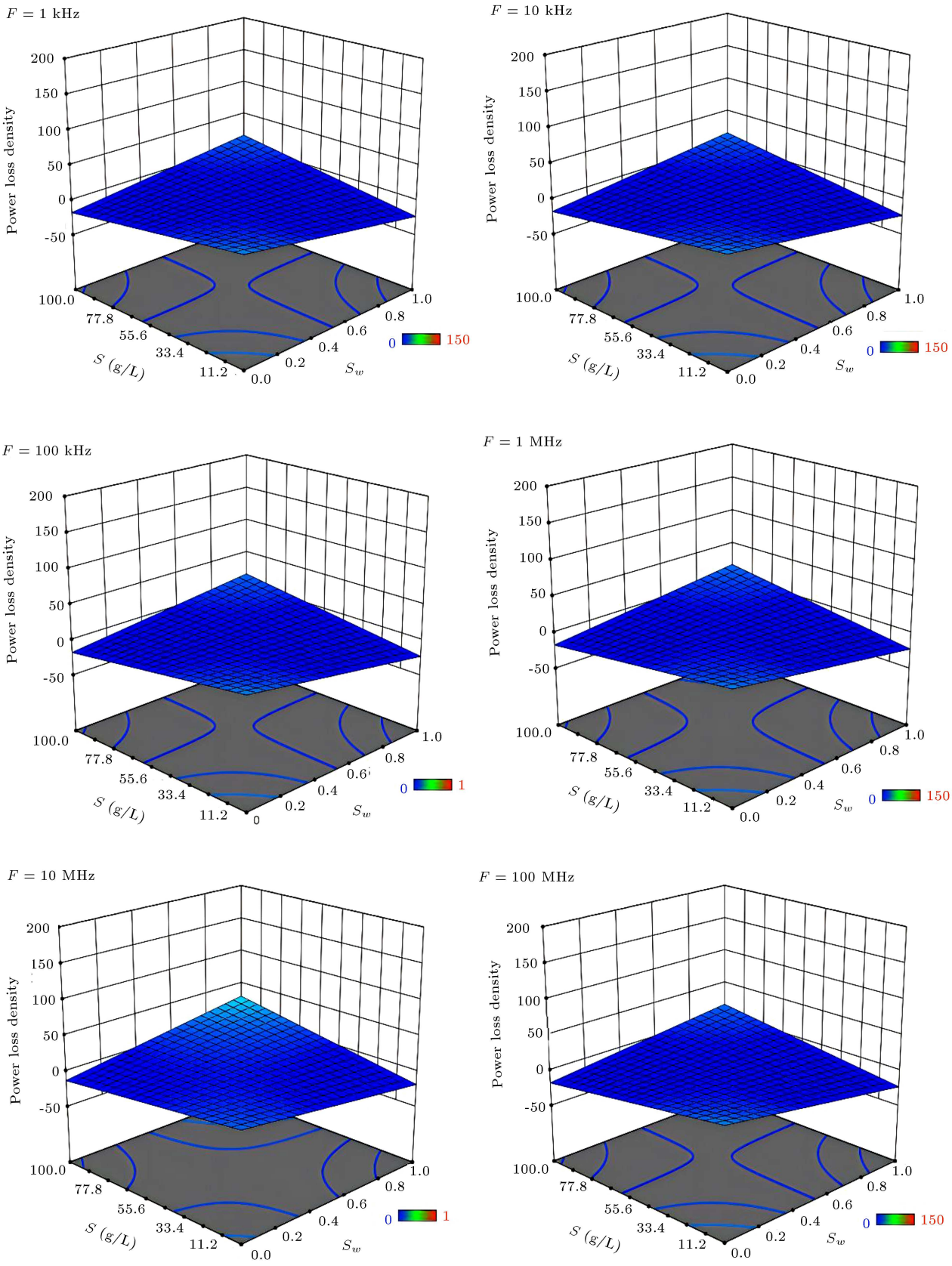

Figure 7. Three-dimensional view of the power loss density at 10–20 cm versus salinity and water saturation at different frequencies.

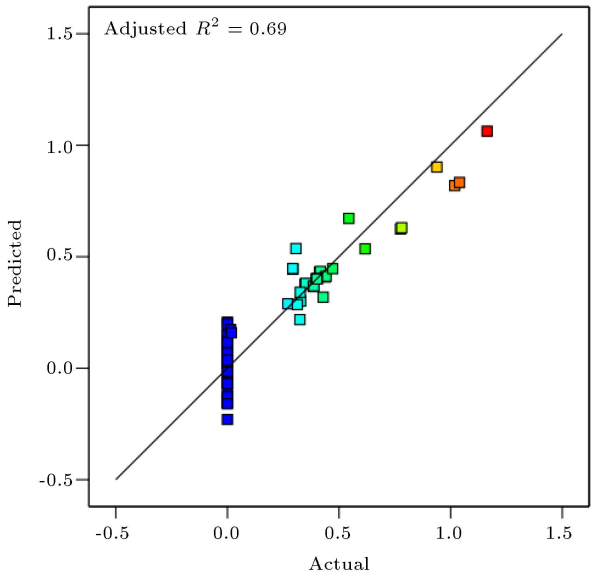

Figure 8. Predicted versus actual data of the power loss density at 20–100 cm far from the wellbore.

the EM wave and brine water saturation were the second and third affecting parameters, respectively. By increasing the distance from the wellbore, the effect of the EM wave frequency increased. From 20–100 cm far from the wellbore, the most affecting factor was the frequency. The reason was the dependency of the EM wave penetration depth to the frequency. Hence, by increasing the distance of the target zone from the wellbore, the frequency became the most important issue;

2. At each frequency, the most power loss density occurred when the salinity and water saturation tended to the maximum value. As could be seen in the 3-dimensional figures, the increment in power loss density increased as the frequency increased to 100 MHz, drastically. A weak peak could be seen when the salinity of the brine water decreased. According to the Stogryn model, increasing the salinity of the water increased the water dielectric, and increasing the dielectric constant brought about greater dissipation of the EM energy. By decreasing the salinity, factors concerning non-water-related parameters appear more efficient in increasing the power loss density;
3. Following an increase in the distance from the wellbore, the power loss density decreased. The maximum power loss density in the section of 5–6 cm was 4300 Watt/m^3 while the maximum one was generally almost 1 Watt/m^3;
4. All of the input factors had a positive coefficient in the proposed correlations by Box-Behnken; hence, all of them enhanced the power loss density of the EM wave around the wellbore. Based on the obtained results in the regions of 5–6 cm, 6–10 cm, 10–20 cm, and 20–100 cm, the increased wave frequency led to greater power loss. As a result, it is more efficient to implement the highest frequency possible and there is no minimum or optimum wave frequency;
5. To the best of our knowledge, it is the first time that CST software is used to simulate the EM waves in the oil and gas industry. The obtained results are not limited to a specific reservoir condition and as a result, it could be used as a guideline for the planning of EM stimulation projects. We do accept that there remain many issues to investigate in this area. Thus, other researchers are encouraged to experimentally study the affecting parameters concerning the EM stimulation.

Acknowledgment

This research did not receive any specific grant from funding agencies in the public, commercial, or not-for-profit sectors.

Nomenclature

p_{ave}	Average Dissipated Power (j/s)
E	Root mean square electric field (V/m)
$\bar{\varepsilon}$	Dielectric constant (Imaginary Part)
ε_0	Dielectric constant (Real Part)
σ	Electric conductivity (S/m)
ω	Radian frequency (rad/s)
V	Medium volume (m^3)
S_w	Water saturation (Dimensionless)
S	Water salinity (g/L)
F	Frequency (Hz)
E_o	Oil dielectric constant (Dimensionless)
E_r	Rock dielectric constant (Dimensionless)
T_i	Initial temperature (°C)
Phi	Porosity (Dimensionless)
ε_∞	Optical dielectric constant of the brine (Dimensionless)
τ	Relaxation time (s)
ε_0^*	Electric field permittivity at free space that is 8.85×10^{-12} (F/m)
j	Current density (A/m^2)
μ	Magnetic permeability (H/m)
H	Magnetic field (Tesla)

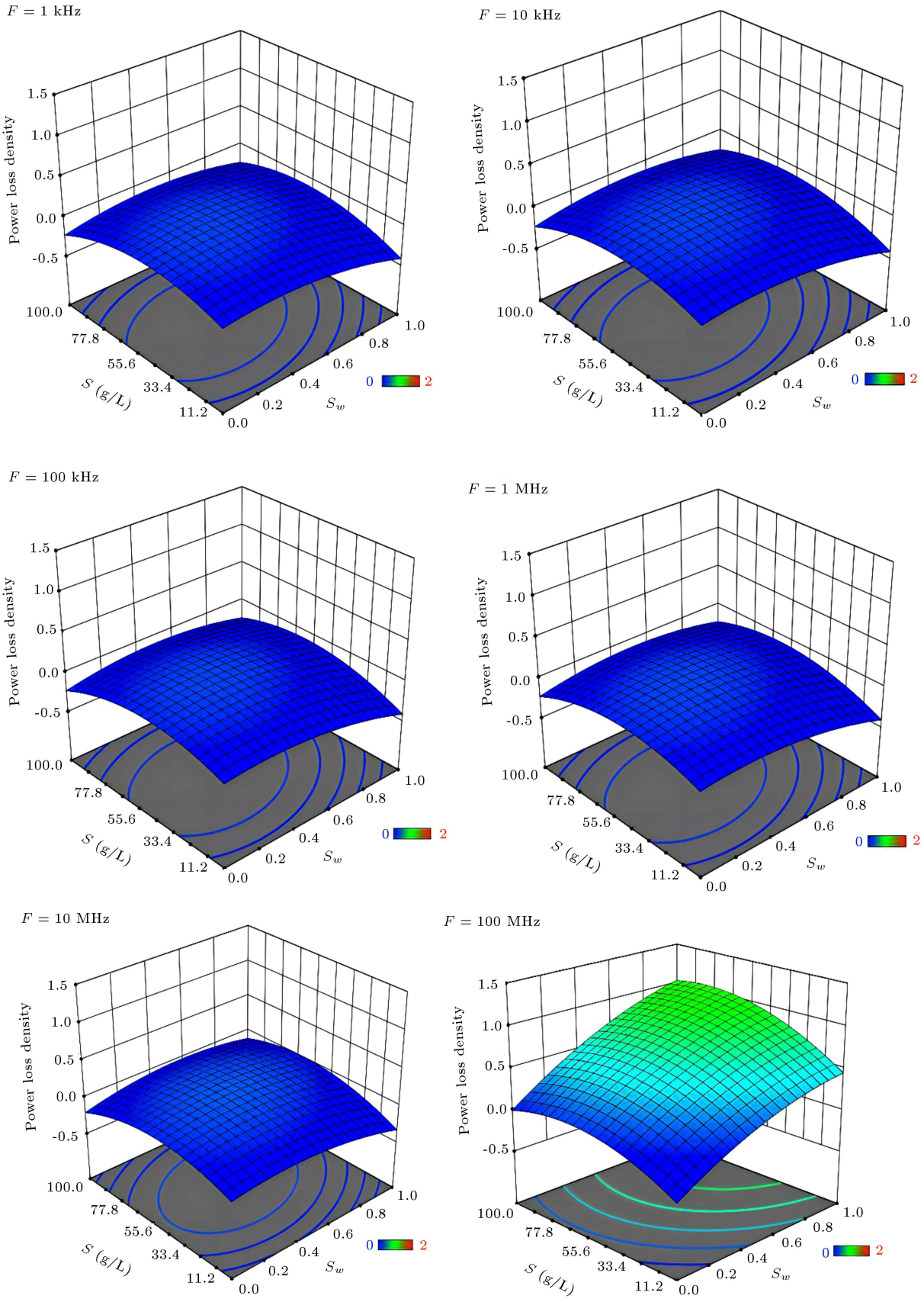

Figure 9. 3-Dimensional view of the power loss density in 20–100 cm versus salinity and water saturation at different frequencies.

References

1. Bahraminejad, H., Khaksar Manshad, A., Riazi, M., et al. "CuO/TiO_2/PAM as a novel introduced hybrid agent for water-oil interfacial tension and wettability optimization in chemical enhanced oil recovery", *Energy and Fuels*, **33**(11), pp. 10547–10560 (2019).
2. Walker, J., Halliday, D., and Resnick, R., *Fundamentals of Physics*, 10th Ed. (2014).
3. Sahni, A., Kumar, M., and Knapp, R.B. "Electromagnetic heating methods for heavy oil reservoirs", *SPE/AAPG West. Reg. Meet.* (2000).
4. Karami, S., Saeedi Dehaghani, A.H., and Hossein Seyed Mousavi, S.A. "Condensate blockage removal using microwave and ultrasonic waves: Discussion on rock mechanical and electrical properties", *J. Pet. Sci. Eng.*, **193**, 107309 (2020).
5. Hakala, J.A., Stanchina, W., Soong, Y., et al. "Influence of frequency, grade, moisture and temperature on Green River oil shale dielectric properties and electromagnetic heating processes", *Fuel Process. Technol.*, **92**(1), pp. 1–12 (2011).
6. Taheri-Shakib, J., Shekarifard, A., and Naderi, H. "The experimental study of effect of microwave heating time on the heavy oil properties: Prospects for heavy oil upgrading", *J. Anal. Appl. Pyrolysis*, **128**, pp. 176–186 (2017).
7. Taheri-Shakib, J., Shekarifard, A., and Naderi, H. "The experimental investigation of effect of microwave and ultrasonic waves on the key characteristics of heavy crude oil", *J. Anal. Appl. Pyrolysis*, **128**, pp. 92–101 (2017).
8. Taheri-Shakib, J., Shekarifard, A., and Naderi, H. "The study of influence of electromagnetic waves on the wettability alteration of oil-wet calcite: Imprints in surface properties", *J. Pet. Sci. Eng.*, **168**, pp. 1–7 (2018).
9. Karami, S., Saeedi Dehaghani, A.H., and Haghighi, M. "Investigation of smart water imbibition assisted with microwave radiation as a novel hybrid method of enhanced oil recovery", *J. Mol. Liq.*, **335**, 116101 (2021).
10. Taheri-Shakib, J., Shekarifard, A., and Naderi, H. "Experimental investigation of comparing electromagnetic and conventional heating effects on the unconventional oil (heavy oil) properties: Based on heating time and upgrading", *Fuel*, **228**, pp. 243–253 (2018).
11. Nasri, Z. and Mozafari, M. "Multivariable statistical analysis and optimization of Iranian heavy crude oil upgrading using microwave technology by response surface methodology (RSM)", *J. Pet. Sci. Eng.*, **161**, pp. 427–444 (2018).
12. Taheri-Shakib, J., Shekarifard, A., and Naderi, H. "Heavy crude oil upgrading using nanoparticles by applying electromagnetic technique", *Fuel*, **232**, pp. 704–711 (2018).
13. Hascakir, B. and Akin, S. "Recovery of Turkish oil shales by electromagnetic heating and determination of the dielectric properties of oil shales by an analytical method", *Energy and Fuels*, pp. 503–509 (2010).
14. El Harfi, K., Mokhlisse, A., Chanâa, M.B., et al. "Pyrolysis of the Moroccan (Tarfaya) oil shales under microwave irradiation", *Fuel*, **79**(7), pp. 733–742 (2000).
15. Ali, H., Soleimani, H., Yahya, N., et al. "Absorption of electromagnetic waves in sandstone saturated with brine and nanofluids for application in enhanced oil recovery", *J. Taibah Univ. Med. Sci.*, **14**(1), pp. 217–226 (2020).
16. Ali, H., Soleimani, H., Yahya, N., et al. "Enhanced oil recovery by using electromagnetic-assisted nanofluids: A review", *J. Mol. Liq.*, **309**, 113095 (2020).
17. Haroun, M., Al Hassan, S., Ansari, A., et al. "Smart nano-EOR process for Abu Dhabi carbonate reservoirs", *Soc. Pet. Eng.-Abu Dhabi Int. Pet. Exhib. Conf. 2012, ADIPEC 2012 - Sustain. Energy Growth People, Responsib. Innov.* (2012).
18. Adil, M., Mohd Zaid, H., Chuan, L.K., et al. "Effect of EM propagation medium on electrorheological characteristics of dielectric nanofluids", *J. Dispers. Sci. Technol.*, **38**(4), pp. 570–576 (2017).
19. Bera, A. and Babadagli, T. "Effect of native and injected nano-particles on the efficiency of heavy oil recovery by radio frequency electromagnetic heating", *J. Pet. Sci. Eng.*, **153**, pp. 244–256 (2017).
20. Soleimani, H., Latiff, N.R.A., Yahya, N., et al. "Synthesis and characterization of yttrium iron Garnet (YIG) Nanoparticles activated by electromagnetic wave in enhanced oil recovery", *J. Nano Res.*, **38**, pp. 40–46 (2016).
21. Robinson, J., Binner, E., Saeid, A., et al. "Microwave processing of Oil Sands and contribution of clay minerals", *Fuel*, **135**, pp. 153–161 (2014).
22. Dassault Systémes, "CST studio suite 2020", *Tech. Data Sheet*, p. 392 (2020).
23. Rudge, Alan W. and Milne, K. (Eds.), *The Handbook of Antenna Design*, **16**, Iet (1982).
24. Punase, A. and Hascakir, B. "Stability determination of asphaltenes through dielectric constant measurements of polar oil fractions", *Energy and Fuels*, **31**(1), pp. 65–72 (2017).
25. Goual, L. "Impedance spectroscopy of petroleum fluids at low frequency", *Energy and Fuels*, **23**(4), pp. 2090–2094 (2009).
26. Persson, K. "Materials data on In2O3 (SG:206) by materials project", *Mater. Proj.*, **N**(p) (2020). https://materialsproject.org/materials/mp-8352/ DOI: 10.17188/1281939

27. Mätzler, C. and Murk, A. "Complex dielectric constant of dry sand in the 0.1 to 2 GHz range", Univ. Bern, Bern (2010). DOI: 10.13140/2.1.2387.9044

28. Wang, S., Sun, Q., Wang, N., et al. "Variation in the dielectric constant of limestone with temperature", *Bull. Eng. Geol. Environ.*, **79**(3), pp. 1394–1355 (2020).

29. Gadani, D.H., Rana, V.A., Bhatnagar, S.P., et al. "Effect of salinity on the dielectric properties of water", *Indian J. Pure Appl. Phys.*, **50**(6), pp. 405–410 (2012).

30. Meissner, T. and Wentz, F.J. "The complex dielectric constant of pure and sea water from microwave satellite observations", *IEEE Trans. Geosci. Remote Sens.*, **42**(9), pp. 1836–1849 (2004).

31. Chaturvedi, P.K., *Microwave, Radar & RF Engineering*, Springer Singapore (2018).

Biographies

Saeed Karami graduated from the Petroleum Department at Petroleum University of Technology and Tarbiat Modares University, Iran. He is now a Research Assistant at Enhanced Oil Recovery Lab and conducts research on various research topics of chemical and petroleum engineering such as oil upgrading and waste management. A part of his research projects is now published in peer-reviewed journals.

Amir Hossein Saeedi Dehaghani received his PhD from Tarbiat Modares University, Iran. He is now an Assistant Professor at the Chemical Engineering Department of Tarbiat Modares University. His research interests include enhanced oil recovery and organic scale in petroleum industry. He has published more than 80 research papers in peer-reviewed journals.